

Article

Hybrid Data-Driven and Explainable Modeling of Compressive Strength in GGBFS–MRP Concrete with Environmental Optimization

Zahraa Raheem¹, Zainab Mohammed¹, Zarya Barzan¹ and Ahmed Salih Mohammed^{2,*}¹ Civil Engineering Department, College of Engineering, The American University of Iraq-Sulaimani (AUIS), Sulaimani 46001, Iraq² Civil Engineering Department, College of Engineering, University of Sulaimani, Sulaimani 46001, Iraq* Correspondence: ahmed.mohammed@univsul.edu.iq; Tel.: +00964-7701588695**How To Cite:** Raheem, Z.; Mohammed, Z.; Barzan, Z.; et al. Hybrid Data-Driven and Explainable Modeling of Compressive Strength in GGBFS–MRP Concrete with Environmental Optimization. *Bulletin of Computational Intelligence* 2026, 2(1), 13–30. <https://doi.org/10.53941/bci.2026.100002>

Received: 2 October 2025

Revised: 12 November 2025

Accepted: 14 November 2025

Published: 5 January 2026

Abstract: The production of concrete is expensive, energy-intensive, and a significant source of carbon emissions, with energy use accounting for 30–40% of production costs. Since micronised rubber powder (MRP) and ground granulated blast furnace slag (GGBFS) are industrial byproducts of the rubber and steel industries, respectively, they offer sustainable substitutes. The compressive strength (CS), a crucial measure of structural performance, of GGBFS-MRP modified concrete is examined in this work. Five predictive models Linear Regression (LR), Non-Linear Regression (NLR), Multiple Linear Regression (MLR), M5P-tree, and Artificial Neural Network (ANN) were used to analyse a total of 135 samples. CS varied from 25.01 to 59.27 MPa, while the input variables were cement content (325–425 kg/m³), water-to-binder ratio (0.35–0.45), GGBFS (0–40%), MRP (0–5%), fine aggregate (905–1105 kg/m³), coarse aggregate (711–1082 kg/m³), and curing time (7–91 days). The ANN model outperformed the M5P-tree model in terms of predictive accuracy. Sensitivity analysis revealed that the three most important factors influencing CS were curing time, MRP dosage, and GGBFS content. These findings provide reliable predictive models and insights into optimizing sustainable GGBFS-MRP concrete mixtures.

Keywords: ground granulated blast furnace slag; micronized rubber powder; compressive strength; age; predictive models; sustainability

1. Introduction

Cement industries are known to be high-energy-consuming and high-carbon-emitting sectors, requiring sustainability measures to reduce greenhouse gas emissions [1,2]. The manufacturing process is the primary culprit, utilizing thermal energy during the burning process and electrical energy for grinding the cement itself. These energy costs have been estimated to contribute to 50–60% of total cement production costs [1]. Blast furnace slag, a byproduct of the steel industry, can be used as a partial replacement for cement in concrete production, thereby lowering construction costs and simultaneously recycling waste products from other sectors—essentially acting as a free source of energy [3]. On the other hand, the automobile industry has been consuming and discarding millions of rubber tires worldwide, a trend that is accelerating as the industry expands. Over 50% of these tires are scrapped, landfilled, or discarded with no further treatment. However, these tires can be used as fuel in the cement industry, as a partial replacement to coal, or within the interests of this article, they can be recycled in the form of crumb rubber or rubber powder and used as an additive in concrete production [3–5]. Both of these additives, blast furnace slag and tire rubber, offer environmental and ecological benefits as recyclable materials, making desirable contributions to concrete production and its characteristics.



The focus of this paper is on concrete modified using ground granulated blast furnace slag (GGBFS) and micronized rubber powder (MRP) as partial cement replacements. GGBFS is a byproduct of steel production and possesses the property of not reacting to water, which is notable because slag's hydration process is similar to cement, and slag-modified concrete is less penetrable to water as opposed to non-modified and naturally hardened concrete. MRP is recycled from post-industrial rubber products, such as automobile tires, and is a relatively soft material. This means that MRP typically decreases the mechanical properties of concrete modified by it [6]. However, little research is available on concrete simultaneously modified by both additives, and the relationship between these two additives will affect the final product, which is of interest to this paper.

Independent parameters include: MRP, GGBFS, cement, water-to-binder ratio (W/B), fine aggregate (FA), coarse aggregate (CA), and time. The most critical and relevant dependent variable is compressive strength (CS), but tensile strength (TS) and flexural strength (FS) are also of interest. CS is a critical property of concrete in construction. To properly evaluate and predict the impact of these variables on CS, this paper employs machine learning and modeling techniques. Data were collected from 135 samples of GGBFS-MRP-modified concrete and split into 70% for training and 30% for testing. Five main statistical predictive models were used in this study; each was analyzed and compared with the others to determine which was most consistent and accurate. These include linear regression (LR), non-linear regression (NLR), multi-line regression (MLR), M5P-tree models, and artificial neural networks (ANNs).

1.1. Research Objectives

This study aims to examine the effects of cement, W/B, FA, CA, and time on the CS of GGBFS-MRP-modified concrete. It seeks to achieve this through a thorough analysis of the accuracy and limitations of the various models used to predict CS, using data from carefully selected prior studies. The following are the main objectives:

- I. Conduct a thorough and diligent sensitivity analysis to determine the significance of different variables on the CS of GGBFS-MRP modified concrete.
- II. Encourage and support the use of recyclable materials in concrete production to allow for cleaner and more sustainable construction.
- III. Develop measurement methods in the form of predictive computing models to accurately forecast the CS of 135 compositions of GGBFS-MRP modified concrete.
- IV. Determine the most reliable, accurate, and consistent modeling method to predict CS among the LR, NLR, MLR, ANN, and M5P-tree models by using statistical analysis.

1.2. Dataset Description

A respected study by Amiri et al. utilized data from 135 concrete samples with varying mixture proportions to predict the compressive strength (CS) of GGBFS-MRP-modified concrete. The flowchart, data scatter for dependent and independent variables are presented in Figures 1–3. The following seven input variables were considered: cement content, water-to-binder ratio (W/B), GGBFS, MRP, fine aggregate (FA), coarse aggregate (CA), and curing time. GGBFS, MRP, and curing time were found to be the most critical factors that affected CS. Cement, W/B, FA, and CA had a lesser effect. The correlation matrix of the variables is shown in Figure 4. The values range from -1 to 1 . Negative values indicate inverse relationships, while positive values indicate direct relationships; values close to zero indicate little correlation.

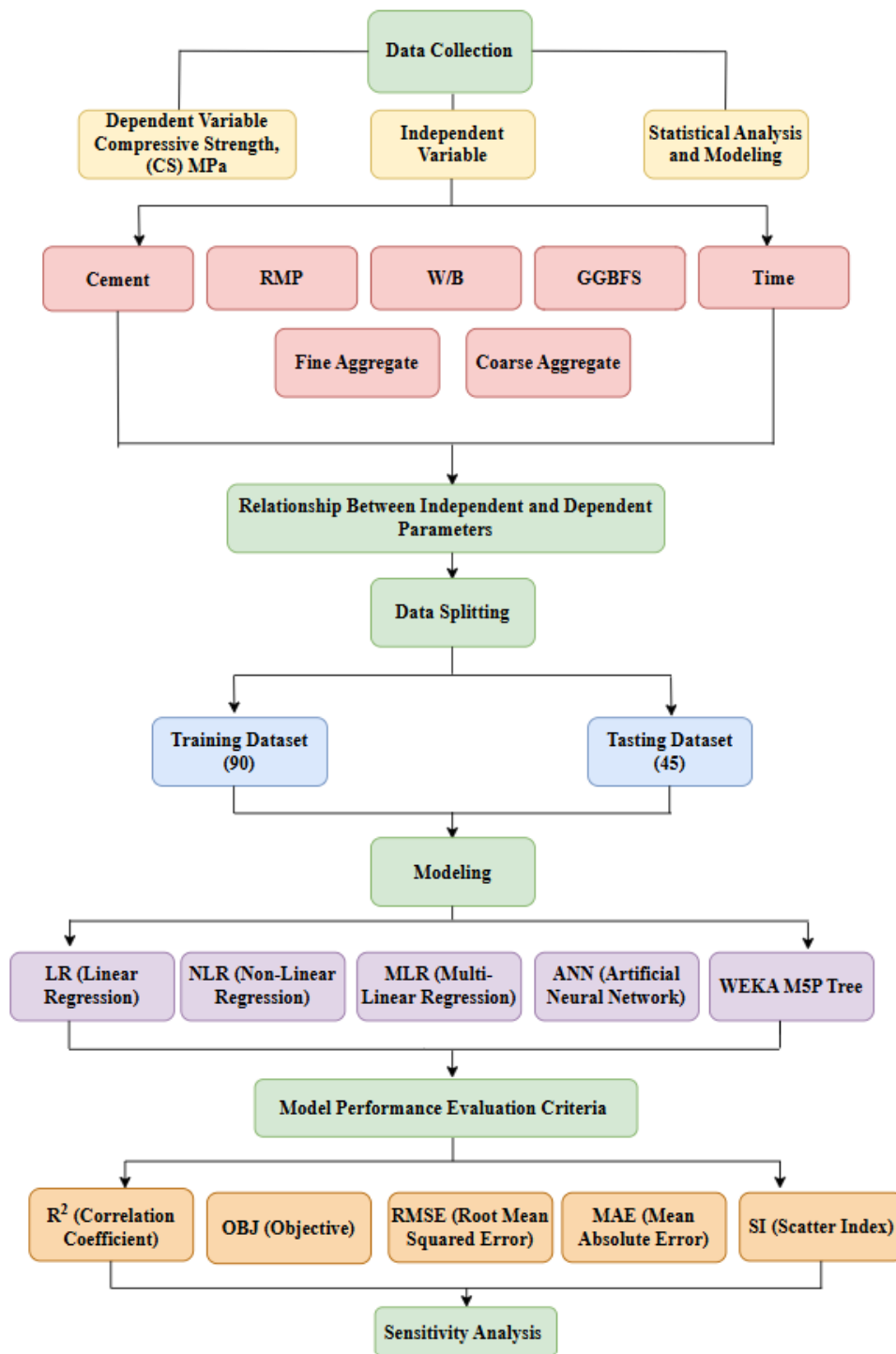
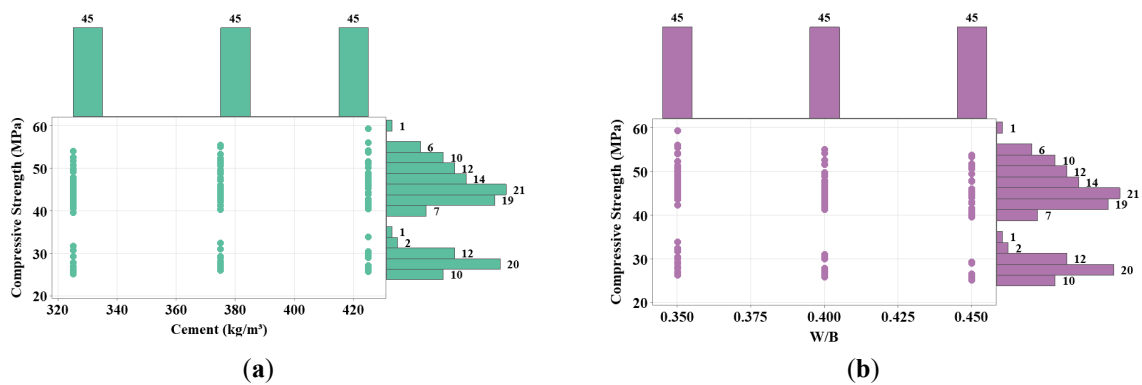


Figure 1. Flowchart diagram for the conducted study.



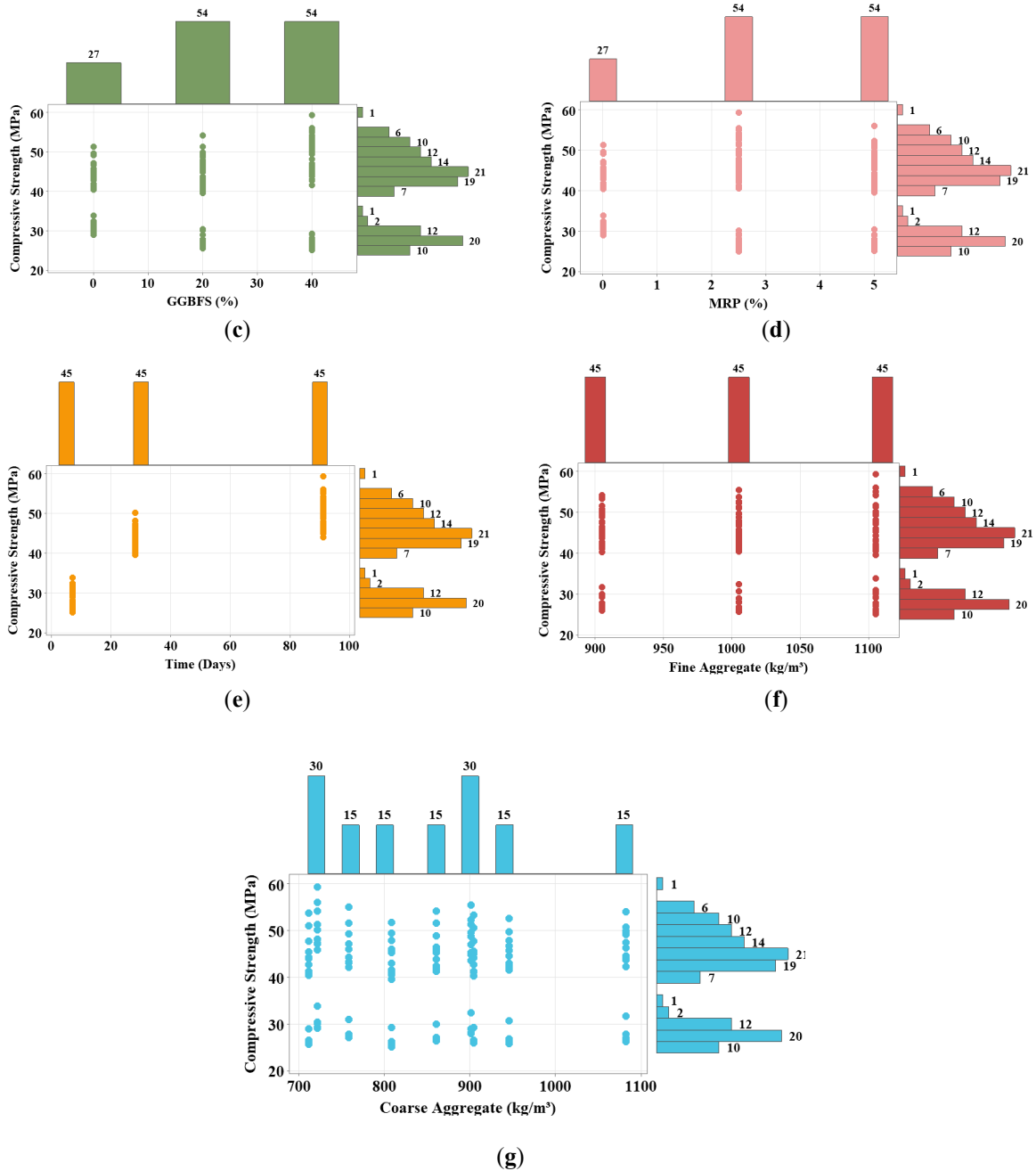


Figure 2. Marginal plot between compressive strength of recycled aggregate concrete and (a) Cement (kg/m³); (b) (W/B); (c) GGBFS (%); (d) MRP (%); (e) Time (Days); (f) Fine Aggregate (kg/m³); (g) Coarse Aggregate (kg/m³).

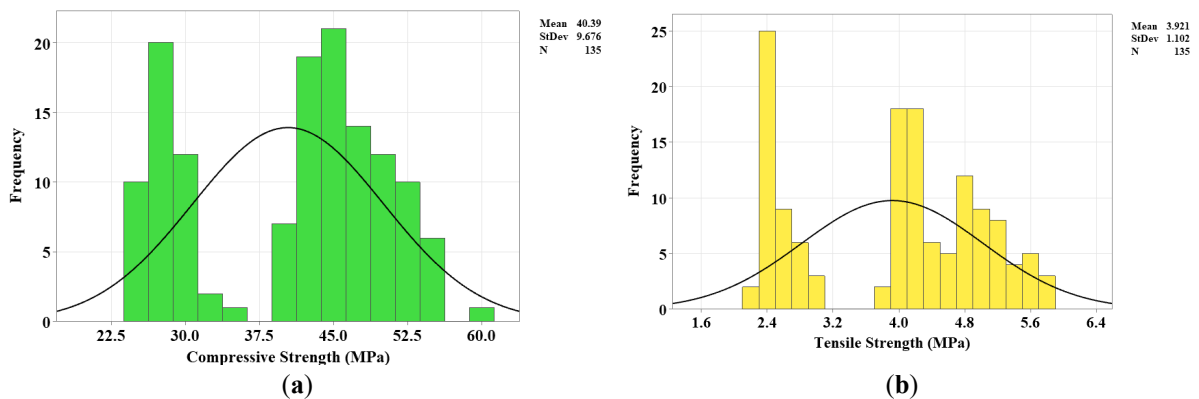


Figure 3. Frequency graph for concrete with GGBFS and MRP: (a) Compressive strength, CS (MPa); (b) Tensile strength, TS (MPa).

	Cement	W/B	GGBFS %	MRP %	Time	FA	CA	CS	TS	FS
Cement (kg/m ³)	1.00									
W/B	-0.03	1.00								
GGBF%	0.05	0.05	1.00							1.00
MRP%	0.01	0.09	0.61	1.00						0.50
Time (day)	0.03	0.05	-0.01	0.03	1.00					0.00
FA (kg/m ³)	0.00	-0.05	0.00	-0.02	0.07	1.00				-0.50
CA (kg/m ³)	-0.63	-0.30	-0.05	-0.03	-0.08	-0.69	1.00			-1.00
CS (MPa)	0.12	-0.11	0.03	-0.07	0.83	0.14	-0.14	1.00		
TS (MPa)	0.11	0.01	0.04	-0.05	0.89	0.11	-0.15	0.99	1.00	
FS (MPa)	0.16	-0.14	0.07	-0.07	0.83	0.15	-0.16	0.99	0.98	1.00

Figure 4. Correlation matrix for the correlation between all the variables.

2. Methodology

Figure 1 illustrates the methodology employed in this study and provides a detailed overview of the procedures implemented. To investigate the mechanical characteristics of GGBFS-MRP-based concrete, a total of 135 samples were obtained from the survey by research [6]. To ensure accuracy and consistency in model development, the dataset was divided into training (90 samples, 70%) and testing (45 samples, 30%) subsets. The dataset includes the following parameters: cement content, water-to-binder ratio (W/B), micronized rubber powder (MRP), ground granulated blast-furnace slag (GGBFS), fine aggregate (FA), micronized rubber powder (MRP), coarse aggregate (CA), and curing time. The primary objective of the study was to predict the compressive strength (CS) of GGBFS-MRP concrete using five predictive statistical models: linear regression (LR), Non-Linear Regression (NLR), multiple linear regression (MLR), Artificial Neural Network (ANN), and M5P-tree model. A sensitivity analysis was performed to evaluate the influence of input parameters on CS, revealing that curing time, GGBFS content, and MRP dosage have the most significant impact on compressive strength predictions.

2.1. Data Statistics

The acquired dataset underwent statistical analysis to detect interactions and correlations between the complete set of independent variables and the dependent variable (inputs and outputs). Figure 2 illustrates marginal plots of the compressive strength (CS) of GGBFS-MRP-based concrete (dependent variable) against various concrete parameters (independent variables). Table 1 presents the statistical attributes of the experimental dataset used to model the mechanical performance of GGBFS-MRP concrete. The dataset comprises seven input variables: cement content, water-to-binder ratio (W/B), ground granulated blast furnace slag (GGBFS) content, marble residue powder (MRP) content, curing time, fine aggregate, and coarse aggregate, along with three output responses: compressive strength, tensile strength, and flexural strength. The cement concentration ranges from 325 kg/m³ to 425 kg/m³, with an average of 375 kg/m³, indicating that most combinations were formulated for standard, moderate-strength concrete. The modest standard deviation (40.98) and variance (1679.10) indicate a regulated fluctuation in cement dose, ensuring experimental uniformity. The water-to-binder ratio (W/B) ranges from 0.35 to 0.45, with an average of 0.40, indicating the practical constraints for achieving workable, yet thick, concrete. The minimal variance (0.0017) indicates that the mixtures were formulated within a limited range to provide comparability among various binder combinations. The GGBFS concentration ranges significantly from 0% to 40%, with an average of 23.94% and a considerable standard deviation of 15.02, indicating extensive variation in slag replacement levels. The MRP concentration varies from 0% to 5%, with an average of 2.99%, indicating a focus on the reasonable integration of marble powder to achieve a balance between sustainability and mechanical performance. The cure duration ranges from 7 to 91 days, with an average of 42.10 days and a substantial variation of 1283.51, reflecting both early-age and long-term strength development characteristics. This variance facilitates the modeling of time-dependent strength growth with sufficient generalization. The fine aggregate has a range of 905–1105 kg/m³ (mean = 1005 kg/m³), whereas the coarse aggregate varies from 711–1082 kg/m³ (mean = 855.06 kg/m³). The elevated standard deviation of coarse aggregate (113.20) relative to fine aggregate (81.95) indicates greater variability in the coarse fraction, presumably due to the mix optimization for workability and density. The compressive strength of the target variables ranges from 25.01 to 59.27 MPa, with an average of 40.42 MPa, indicating the presence of both medium and high-strength concretes. The moderate variance (93.63) indicates that the dataset encompasses a sufficiently varied range of strengths, making it suitable for machine learning research. The tensile strength (2.25–5.82 MPa; mean = 3.92 MPa) and flexural strength (3.32–7.21 MPa; mean = 4.97 MPa)

exhibit comparable dispersion patterns and correlate with standard empirical correlations for compressive strength. The dataset exhibits balanced variability and representativeness, facilitating robust statistical learning and mitigating overfitting. The variable distribution verifies that the experimental design accurately reflects the impact of binder composition, aggregate ratios, and curing age on the mechanical properties of sustainable GGBFS–MRP concrete. Table 2 presents the model performance evaluation.

Figure 3 shows two frequency histograms: (a) displays the frequency distribution of the obtained compressive strength (CS); and (b) shows the frequency distribution of the measured tensile strength (TS). Figure 4 illustrates the correlation between the independent and dependent variables in the dataset for GGBFS–MRP-based concrete. In this study, each parameter has been evaluated for its minimum, maximum, mean, median, mode, standard deviation, skewness, and variance. Minimum and maximum values represent the smallest and largest values for each parameter. The mean indicates the average value, the median is the middle value, and the mode is the most frequently occurring value in the dataset. The standard deviation measures how much each value deviates from the mean, while the variance reflects the overall spread of the data. Table 1 presents the statistical analysis performed on all independent and dependent variables [7]. The study investigated the non-linear degradation of GFRP rebars in terms of tensile strength retention (TSR), considering five key factors: bar diameter, fiber volume fraction, pH, temperature, and conditioning duration. Hybrid artificial neural network (ANN) models, enhanced with particle swarm optimization (PSO), grey wolf optimization (GWO), and marine predators' algorithm (MPA), were developed to predict TSR under different environmental conditions. Statistical, sensitivity, and uncertainty analyses showed that the ANN-GWO model outperformed the others, achieving the highest correlation and lowest prediction errors. Environmental reduction factors (CE) were computed, indicating that larger bar diameters experienced less deterioration. The study emphasizes the need to consider bar size and environmental conditions in the construction of GFRP-reinforced concrete buildings, advocating a CE of around 0.75 at 28 °C in strongly alkaline environments. The study demonstrates the importance of considering bar size and environmental conditions when constructing GFRP-reinforced concrete structures. It suggests that CE should be about 0.75 at 28 °C in very alkaline environments [8].

Table 1. Statistical analysis for dependent and independent variables.

Variable	Units	Min.	Max.	Mean	Median	Mode	Standard Deviation	Variance
Cement	kg/m ³	325	425	375	375	325	40.98	1679.10
W/B	-	0.35	0.45	0.4	0.4	0.45	0.04	0.0017
GGBFS	%	0	40	23.94	20	20	15.02	225.67
MRP	%	0	5	2.99	2.5	5	1.88	3.53
Time	Days	7	91	42.10	28	7	35.83	1283.51
Fine Aggregate	kg/m ³	905	1105	1005	1005	1105	81.95	6716.42
Coarse Aggregate	kg/m ³	711	1082	855.06	860	808	113.20	12,814.73
Compressive Strength	MPa	25.01	59.27	40.42	43.18	41.26	9.68	93.63
Tensile Strength	MPa	2.25	5.82	3.92	4.11	2.44	1.10	1.22
Flexural Strength	MPa	3.32	7.21	4.97	5.12	3.59	0.97	0.94

Table 2. A showcase of the assessment criteria used to evaluate the performance of the five models.

Model	Figure	Equation	Training			Testing		
			R ²	RMSE (MPa)	MAE (MPa)	R ²	RMSE (MPa)	MAE (MPa)
LR	5	1	0.745	4.82	4.21	0.723	4.93	4.42
NLR	6	2	0.923	2.64	2.33	0.923	2.60	2.19
MLR	7	3	0.910	2.87	2.47	0.908	2.84	2.60
ANN	8	-	0.999	0.32	0.26	0.999	0.28	0.23
M5P Tree	10	-	0.982	1.49	1.25	0.954	2.17	1.92

2.2. Modeling Techniques

Various modeling techniques are used in this study to explore the relationship between independent and dependent variables. To ensure accurate data analysis, the dataset was divided into training and testing sets [9,10]. The training set served as the primary dataset for model development, while the testing set was used to evaluate the model's consistency and validity. As shown in Figure 4, the correlation matrix indicates that the compressive strength (CS) of GGBFS–MRP-based concrete is strongly influenced by curing time, with a correlation coefficient of 0.83. Conversely, the matrix indicates low correlations between CS and the other independent variables. For instance, the correlation coefficients are 0.12 for cement, −0.11 for the water-to-binder ratio (W/B), 0.03 for ground

granulated blast-furnace slag (GGBFS), -0.07 for micronized rubber powder (MRP), 0.14 for fine aggregate (FA), and -0.14 for coarse aggregate (CA). Furthermore, as shown in Figure 4, there are strong correlations between CS and the other dependent variables, with correlation coefficients of 0.99 for both tensile strength (TS) and flexural strength (FS). Based on the collected data, five statistical models were developed to estimate the CS of GGBFS-MRP-based concrete. The accuracy and reliability of these models' predictions were assessed using multiple performance metrics, including R^2 , RMSE, MAE, SI, and OBJ, which will be discussed and explained in more detail later.

2.2.1. Linear Regression Model

Linear regression (LR) is a baseline statistical modeling technique commonly used in engineering to explore and quantify the relationship between a dependent variable and one or more independent variables via a linear function. In the present study, LR was utilized to predict the compressive strength (CS) of concrete incorporating various materials and parameters. These include cement content, water-to-binder ratio (W/B), ground granulated blast furnace slag (GGBFS), micronized rubber powder (MRP), curing time (T), fine aggregate (FA), and coarse aggregate (CA). The model assumes that each independent variable contributes linearly and additively to the response.

While linear regression offers a clear, straightforward framework, its predictive accuracy may be limited when nonlinear or complex interactions among variables are present. Nevertheless, it remains a useful baseline model due to its ease of implementation and transparency in interpreting the influence of each input parameter on the output response [11].

The developed linear regression equation is expressed as:

$$CS (MPa) = \beta_1(C) + \beta_2(W/B) + \beta_3(GGBFS) + \beta_4(MRP) + \beta_5(T) + \beta_6(FA) + \beta_7(CA) \quad (1)$$

The independent parameters are cement (CT), water/binder (W/B), cement (C), slag ($GGBFS$), (MRP), (Time), fine aggregate (FA), and coarse aggregate (CA). The dependent variable is compressive strength (CS). Moreover, β_1 through β_7 are the parameters.

2.2.2. Non-Linear Regression Model

In this study, NLR was applied using seven input variables: cement, water-to-binder ratio (W/B), GGBFS, MRP, curing time (T), fine aggregate (FA), and coarse aggregate (CA). This model was selected to overcome the limitations of linear regression by more effectively capturing non-linear effects in the data [12].

$$CS (MPa) = \beta_0 (C)^{\beta_1} + \beta_2 (L)^{\beta_3} + \beta_4 (F)^{\beta_5} + \beta_6 (FA)^{\beta_7} + \beta_8 (CA)^{\beta_9} + \beta_{10} (W)^{\beta_{11}} + \beta_{12} (SP)^{\beta_{13}} + \beta_{14} \quad (2)$$

where β_0 to β_{14} are regression parameters.

2.2.3. Multi-Linear Regression Model (MLR)

The third model used in this study was the multiple linear regression model (MLR), which was employed to evaluate the compressive strength of GGBFS-MRP-based concrete. A multiple linear regression model aims to assess the impact of multiple independent variables on a dependent variable [13]. Compared to the linear regression model, the multi-linear regression model enables users to work with more variables. Yet, the term 'linear' is still used, given that the response variable is directly associated with a linear combination of the predictor variables [14]. Equation (3) represents the multi-linear regression model, indicating the correlation between GGBFS-MRP-based concrete parameters.

$$CS (MPa) = \beta_0 \times (C)^{\beta_1} \times (W/B)^{\beta_2} \times (GGBFS)^{\beta_3} \times (MRP)^{\beta_4} \times (T)^{\beta_5} \times (FA)^{\beta_6} \times (CA)^{\beta_7} \quad (3)$$

2.2.4. Artificial Neural Network Model (ANN)

Another model for predicting the compressive strength of GGBFS-MRP-based concrete is the artificial neural network (ANN). The ANN model is a nonlinear statistical model used to predict complex correlations among independent and dependent variables. The ANN model is a computational approach modeled after the structure and operation of the human brain. Due to the exceptional capability of ANNs to handle complex and imprecise data, they can be used to identify patterns and trends that are difficult to recognize by either humans or computers [15] (Figure 5).

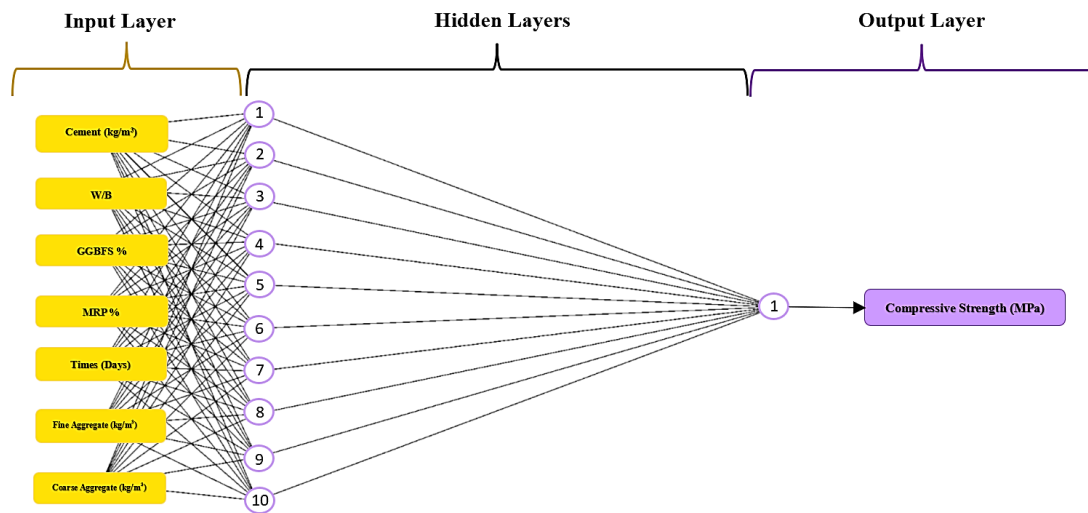


Figure 5. ANN model diagram for the dataset.

2.2.5. M5P Model

The M5P-tree model was the last model applied to estimate the compressive strength of the GGBFS-MRP-based concrete. The M5P-tree is a regression model derived from the M5 algorithm. It incorporates decision trees, which are used to group inputs and outputs and generate a regression equation, in addition to multi-linear regression [16]. Using standard deviation, the M5P-tree model computes error at each node, starting at the bottom of the tree and moving upward [17].

2.3. Performance Evaluation Criteria

To analyze the accuracy and performance of the models, the performance indicators employed in this study include the correlation determination (R^2), Root Mean Square Error (RMSE), Mean Absolute Error (MAE), Scatter Index (SI), and Objective function (OBJ). The R^2 is the proportion of the variance in the dependent variable that can be predicted from the independent variables, with an optimal value of +1 and a worst value of -1∞ [18]. Root Mean Squared Error (RMSE) is defined as the average of the squared differences between the predicted and recorded values. Mean Absolute Error (MAE) is a metric used to evaluate the average magnitude of the absolute error between the predicted and observed values [19]. Mean Absolute Error (MAE) and Root Mean Square Error (RMSE) are widely recommended for evaluating the difference between predicted and actual values [20]. The Scatter Index (SI) helps measure whether the points in the dataset are widely scattered or tightly grouped [21]. The Objective function (OBJ) is a mathematical model used to minimize or maximize decision variables subject to provided constraints [22]. The Equations (4)–(8) specify the statistical evaluation parameters used to calculate each criterion [23–25].

$$R^2 = 1 - \left(\frac{\sum_{i=1}^n (x_i - y_i)^2}{\sum_{i=1}^n (y_i - \bar{y})^2} \right) \tag{4}$$

$$RMSE = \sqrt{\frac{1}{N} \sum_{i=1}^n (x_i - y_i)^2} \tag{5}$$

$$MAE = \frac{1}{N} \sum_{i=1}^n (|x_i - y_i|) \tag{6}$$

$$OBJ = \left(\frac{ntr}{nall} \times \frac{MAEtr + RMSEtr}{Rtr^2 + 1} \right) + \left(\frac{nts}{nall} \times \frac{MAEts + RMSEts}{Rts^2 + 1} \right) \tag{7}$$

$$SI = \frac{RMSE}{\bar{y}} \tag{8}$$

x_i predicted value of CS.

y_i measured value of CS.

\bar{y} stands for the average of the measured CS values.

N indicates the total number of points in the dataset.

n_{tr} denotes the number of points in the training dataset.

n_{ts} demonstrates the number of points in the testing dataset.

n_{all} is the total number of data points for the combined training and testing datasets.

The value of R^2 is between 0 and 1; the ultimate value for R^2 is 1. Therefore, when R^2 is closer to 1, it indicates an excellent prediction; conversely, values closer to 0 indicate a poor prediction. The values for RMSE, MAE, and OBJ range from 0 to infinity; 0 is the optimal value, so the closer the values are to 0, the higher the efficiency of the evaluation process. Concerning SI, when SI value is greater than 0.3 it means that the model has a poor performance, when SI value ranges from 0.2 to 0.3 it indicates a fair performance, when SI is between 0.1 and 0.2 it indicates a good performance, and when it is lower than 0.1 it demonstrates an excellent performance [9,25,26].

3. Results and Discussion

3.1. LR Model

In this study, linear regression (LR) modeling was employed to predict the compressive strength (CS) of concrete incorporating ground granulated blast-furnace slag (GGBFS) and micronized rubber powder (MRP), utilizing seven independent variables. The model's mathematical form is based on linear, constant coefficients representing the direct support of each parameter to the predicted compressive strength.

Although LR provides an elementary, efficient approach, it demonstrated the weakest performance among the models evaluated. The model yielded a coefficient of determination R^2 of 0.745 with a root mean square error RMSE of 4.82 MPa on the training dataset. On the testing dataset, performance declined slightly, with an R^2 of 0.72 and an RMSE of 4.93 MPa. Approximately 85% of the predicted values fell within $\pm 15\%$ of the experimental results.

$$CS = 0.039(C) - 22.9(W/B) + 0.09(GGBFS) - 0.94(MRP) + 0.21(T) + 0.018(FA) + 0.0096(CA)$$

3.2. NLR Model

The non-linear regression (NLR) model was employed to predict the compressive strength (CS) of concrete containing GGBFS and MRP, using the same set of seven input variables. Unlike the linear model, the NLR approach accommodates curved relationships between the input variables and the target output, enabling a more accurate fit of the experimental data.

The model demonstrated significantly improved performance over the linear regression approach. On the training dataset, it achieved an R^2 of 0.923 and an RMSE of 2.64 MPa. The model showed excellent generalization, maintaining an identical R^2 of 0.923 on the test dataset and a slightly lower RMSE of 2.60 MPa. Furthermore, approximately 90% of the predicted values were within $\pm 10\%$ of the actual compressive strength values.

$$CS = -1673.02(C)^{-76.83} + 24.03(W/B)^{-0.42} + 137.71(GGBFS)^{0.02} 280.29(MRP)^{-0.01} \\ + 1854.63(T)^{0.0046} - 1252.31(FA)^{-77.18} - 741.166(CA)^{-85.29} - 2302.95$$

3.3. MLR Model

The multiple linear regression model was used to estimate the compressive strength of various mixtures of GGBFS-MRP-based concrete. As shown in the equation, the model incorporates both linear and exponential parameters, providing more accurate results by capturing the relationship between the independent and dependent variables. Using the training dataset, the equation was developed, and then, to assess the model's effectiveness and accuracy, the same equation was applied to the testing dataset. Figure 5c displays the plot of measured versus predicted compressive strength for the GGBFS-MRP-based concrete using the MLR model. From the MLR model for the training data, $R^2 = 0.909$ and RMSE = 2.686 MPa were obtained; for the testing data, $R^2 = 0.908$ and RMSE = 2.841 MPa were observed. The marginal error of the MLR model ranged between -10% and 10% , indicating that 90% of the data fall between 0.90 and 1.00 on the measured versus predicted compressive strength plot 6).

$$CS \text{ (MPa)} = 20255.4 \times (C)^{-0.23} \times (W/B)^{-0.55} \times (GGBFS)^{0.07} \times (MRP)^{-0.08} \times (T)^{0.21} \times (FA)^{-0.38} \times (CA)^{-0.52}$$

3.4. ANN Model

The artificial neural network (ANN) model was applied to estimate the compressive strength of the GGBFS-MRP-based concrete. The ANN model was applied using Weka software after entering the inputs, outputs, and 10 hidden layers for the training and testing datasets, as shown in the ANN model diagram in Figure 6. The ANN model demonstrated superior performance compared to other models, thanks to its exceptional ability to analyze and uncover patterns in complex data. Figure 5d compares the measured and predicted compressive strengths for the training and testing datasets of GGBFS-MRP-based concrete, obtained using the ANN model. For the training dataset, an R^2 of 0.999 and RMSE of 0.322 MPa were recorded; whereas for the testing dataset, an R^2 of 0.999 and RMSE of 0.279 MPa were recorded. The marginal error was determined to be 5%, which means that about 95% of the data falls between 0.95 and 1.00.

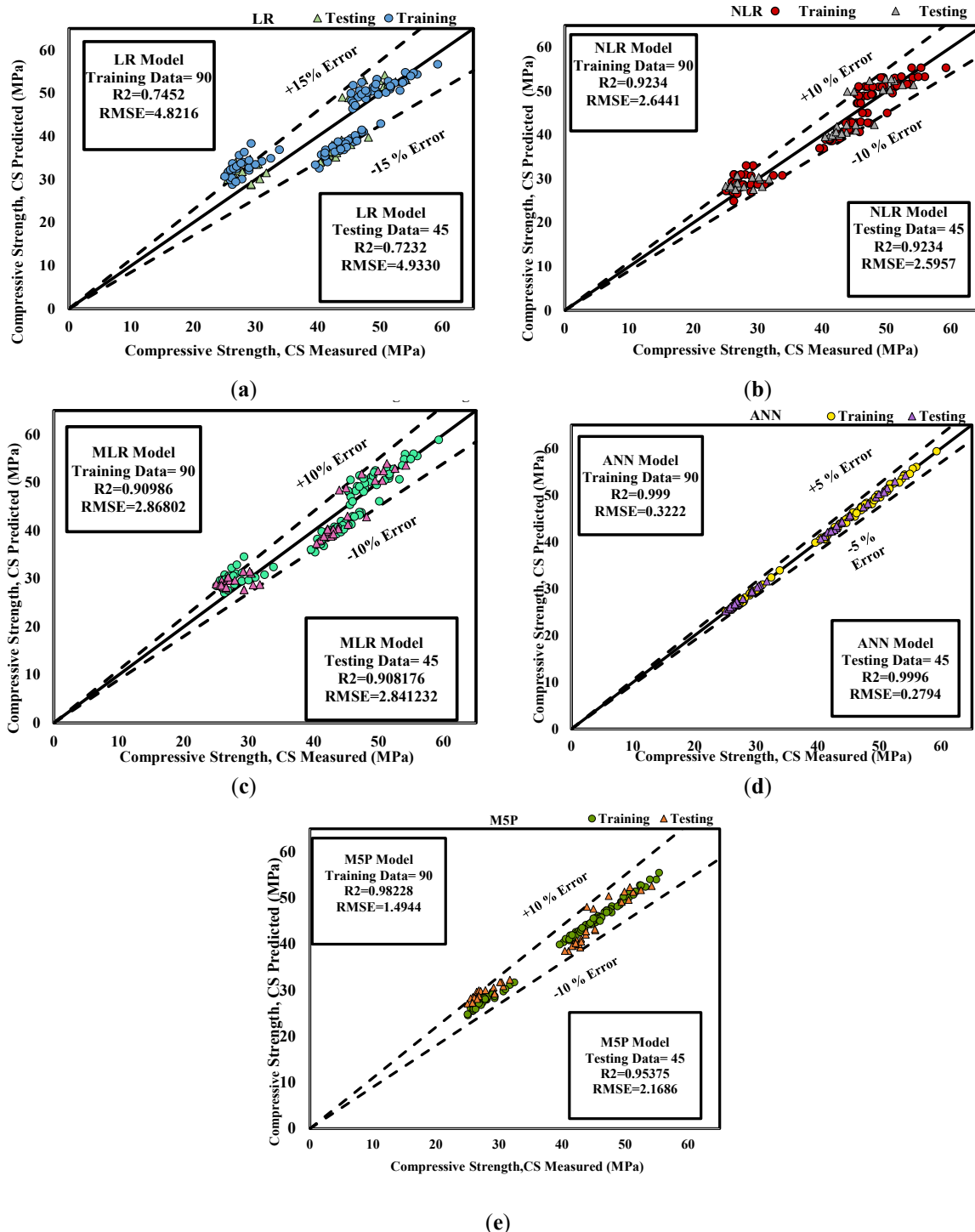


Figure 6. Comparison between measured and predicted compressive strength using: (a) the linear model; (b) the non-linear model; (c) the multi-linear model; (d) the ANN model; (e) the MSP model for training and testing datasets.

3.5. M5P-Tree Model

To calculate the compressive strength of the GGBFS-MRP-based concrete, the M5P-tree model was implemented. The plot of measured versus predicted compressive strength for the training and testing datasets is presented in Figure 5e. Regarding the training datasets, an R-squared value of 0.982 and an RMSE of 1.494 MPa were obtained; while for the testing dataset, an R-squared value of 0.954 and an RMSE of 2.169 MPa were obtained. A margin of error of -10% to 10% was noted, indicating that 90% of the points fall between 0.90 and 1.00. In Figure 7, the M5P Tree is visualized, making the model easier to understand (Figures 8 and 9).

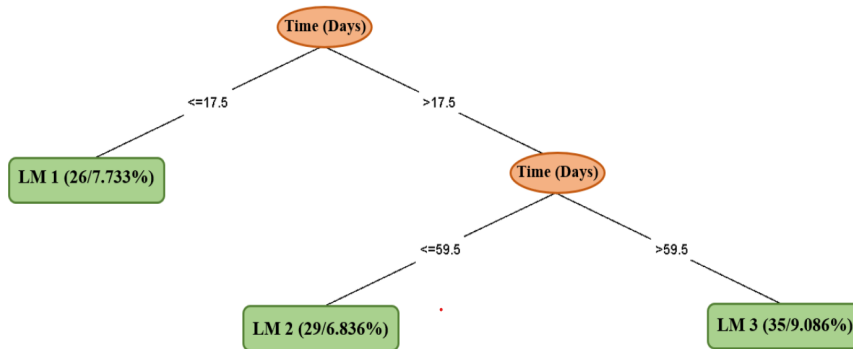


Figure 7. M5P model tree for the dataset.

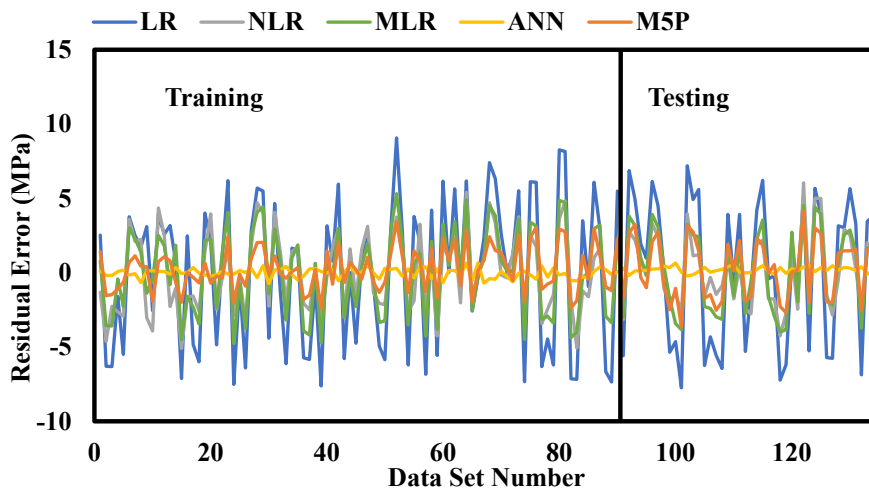
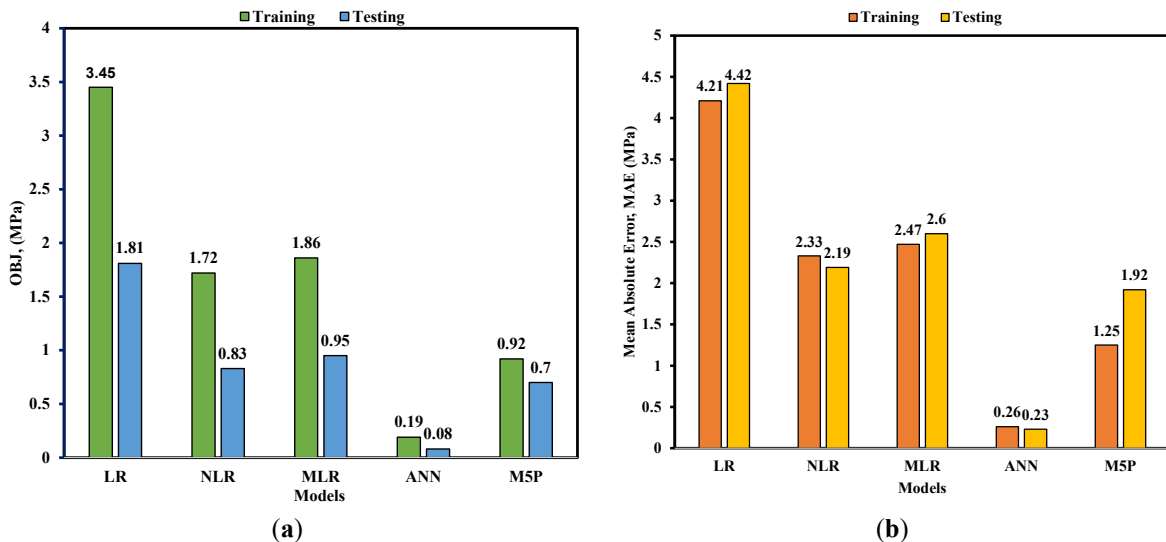


Figure 8. Comparison of residual errors for training and testing for LR, NLR, MLR, ANN, and M5P models.



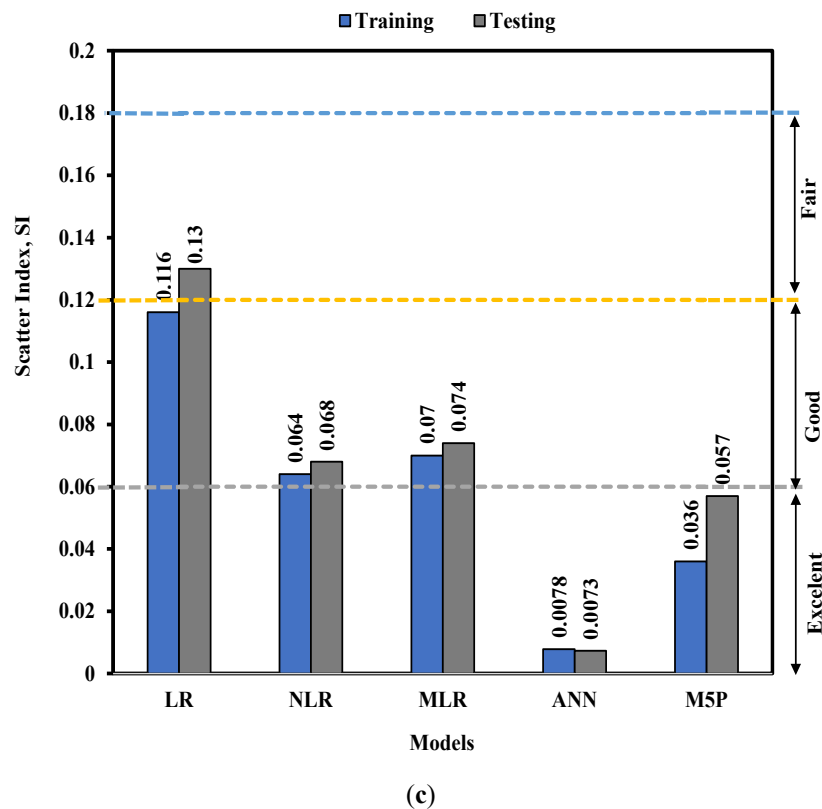


Figure 9. Comparison of (a) Objectives (OBJ); (b) Mean Absolute Error (MAE); and (c) Scatter Index (SI) using training and testing datasets for the five applied models.

4. Affected Parameters

Based on the sensitivity analysis using a Pareto chart, three major factors were identified as influencing the compressive strength (CS) of GGBFS-MRF-based concrete.

4.1. Time

Curing time was the most prevalent factor affecting CS, with the largest standardized effect, approximately 19.8. This input plays a vital role in the progress of hydration products, particularly calcium-silicate-hydrate (C-S-H), which strengthens the concrete matrix. As hydration continues over longer curing times, the concrete becomes denser. This is especially significant for mixtures that incorporate supplementary materials, such as GGBFS. A researcher explained that extended curing leads to better microstructural development and improved mechanical properties [27], while other research emphasized that the strength of blended concrete continues to increase beyond the standard 28-day curing period, highlighting the long-term benefits of extended curing durations [28].

4.2. GGBFS

The second important factor was the percentage of Ground-Granulated Blast-Furnace Slag (GGBFS). GGBFS is recognized for its latent hydraulic features that enhance the short- and long-term strength of concrete. Its fine particles inject the voids between cement grains and react with calcium hydroxide to shape additional C-S-H gel. This dual action improves the packing density and reduces porosity. According to a study [29], the use of GGBFS results in denser concrete with enhanced durability. A study found that increasing the GGBFS dosage improves compressive strength through its pozzolanic and filler effects, especially in well-cured mixtures [30].

4.3. MRP (%)

Although Micronized Rubber Powder (MRP) showed a lower standardized effect than time and GGBFS, it still had an apparent impact. MRP contributes to sustainability by partially replacing cement or filler materials. When processed correctly, especially when fine, it can improve packing density and reduce water demand. A researcher noted that the fineness of MRP allows it to participate in secondary hydration reactions, indirectly improving strength [31]. Meanwhile, another study found that although MRP may reduce early-age strength, its

long-term effects can be neutral or slightly positive when incorporated in moderate proportions, especially in blended systems [32].

5. Model Comparison

Five predictive models, Linear Regression (LR), Non-linear Regression (NLR), Multi-linear Regression (MLR), Artificial Neural Network (ANN), and M5P Tree, were constructed to predict the compressive strength of concrete using statistical performance indicators. The ANN model exhibited the highest accuracy across all metrics, achieving an R^2 of 0.999, an RMSE of 0.3222 MPa, an MAE of 0.2604 MPa, a SI of 0.00775, and the lowest OBJ of 0.1945 MPa; 95% of the predicted values fell within $\pm 5\%$ of the actual values.

The M5P Tree model also applied very well, with an R^2 value of 0.9823, RMSE of 1.4944 MPa, MAE of 1.247 MPa, SI of 0.03594, and OBJ of 0.9219 MPa. Approximately 90% of predictions fell within $\pm 10\%$ of the target, aligning with the high accuracy in compressive strength, albeit with a marginally higher deviation than the ANN.

In contrast, Linear Regression (LR) showed the weakest performance in terms of R^2 , highlighting its limited ability to represent complex relationships in the dataset. The Multi-Linear Regression (MLR) and Non-Linear Regression (NLR) offered acceptable improvements, yet their predictive strength persisted relatively constrained.

6. Sensitivity Investigation

In this study, a sensitivity analysis was conducted to investigate the effect of each independent variable on the compressive strength of GGBFS-MRP-based concrete. Accordingly, a Pareto chart was created to determine the sensitivity index of each independent variable. The results revealed that the independent variables with the greatest impact on CS of GGBFS-MRP-based concrete, ranked from highest to lowest, are curing time, GGBFS, and MRP, as shown in Figure 10. The curing time showed a standardized effect value of 18.33, GGBFS indicated a value of 2.36, and MRP displayed a value of 2.07. The other independent variables, including cement, fine aggregate (FA), coarse aggregate (CA), and water-to-binder ratio (W/B), did not have a significant impact on CS prediction, with standardized effect sizes of 0.66, 0.65, 0.60, and 0.32, respectively.

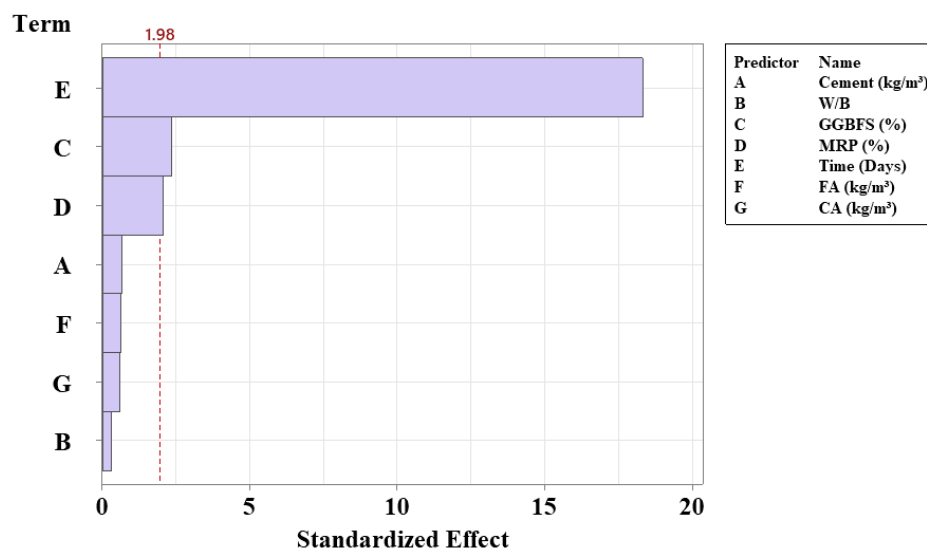


Figure 10. Sensitivity chart (Pareto chart) showing the standardized effects of each independent variable on Compressive strength, CS.

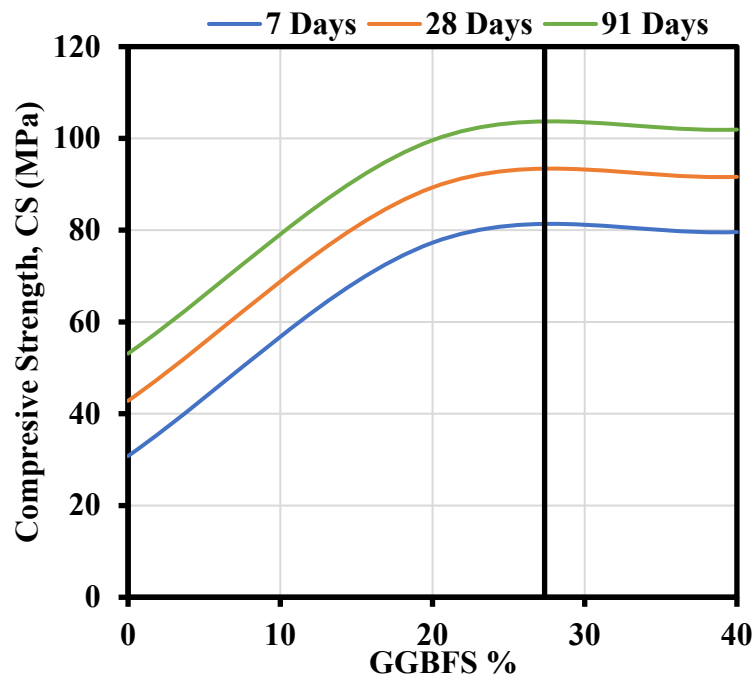
The concrete containing 20 percent GGBFS at curing times of 7 and 28 days exhibits lower compressive strength than the concrete without GGBFS. When the GGBFS percentage is increased to 40 percent, for the same curing time, the concrete shows a higher reduction in its compressive strength. However, at 91 days curing and beyond, higher GGBFS content results in a higher compressive strength [6]. It was reported that adding rubber powder to concrete reduces compressive strength; however, GGBFS mitigates this negative impact [33].

7. Optimum Compressive Strength Investigation

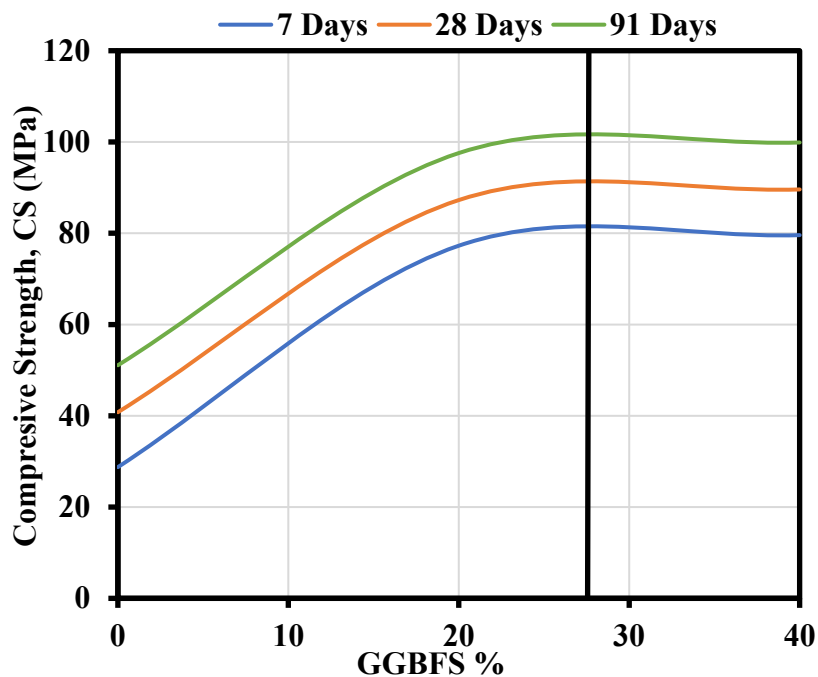
The non-linear model has been confirmed as the best-performing method for this research; therefore, it was implemented to optimize the compressive strength (CS) of the GGBFS-MRP-based concrete. As shown in Figure 11a,

the dataset was fixed on the minimum value for the parameters as listed: 325 (kg/m^3) of cement content, water-to-binder ratio (W/B) of 0.35, 0% MRP replacement, 905 (kg/m^3) fine aggregate content, and 808 (kg/m^3) coarse aggregate content. This was achieved by varying the GGBFS content to assess its impact on compressive strength at 7, 28, and 91 days of curing. It was found that the compressive strength increased with increasing GGBFS until it reached its optimum value of 101.91 (MPa) at 40% of GGBFS and a curing time of 91 days. In Figure 11b, the same procedure was performed, but with selecting the average values of the parameters as follows: 375 (kg/m^3) of cement content, W/B of 0.4, 1005 (kg/m^3) fine aggregate content, and 854.44 (kg/m^3) coarse aggregate content. It was detected that, at a curing age of 91 days and 40% of GGBFS, the maximum value of compressive strength approached 99.89 (MPa). In Figure 11c as a final attempt to find the optimum value of compressive strength, the dataset was set to the maximum value of the parameters in the following manner: 425 (kg/m^3) of cement content, water-to-binder ratio (W/B) of 0.45, 1105 (kg/m^3) fine aggregate content, and 1082 (kg/m^3) coarse aggregate content. The optimum compressive strength was indicated to be 98.19 (MPa) at a curing time of 91 days and 40% of GGBFS replacement.

The compressive strength of the concrete was corrected with tensile and flexural strength as shown in Figure 12.



(a)



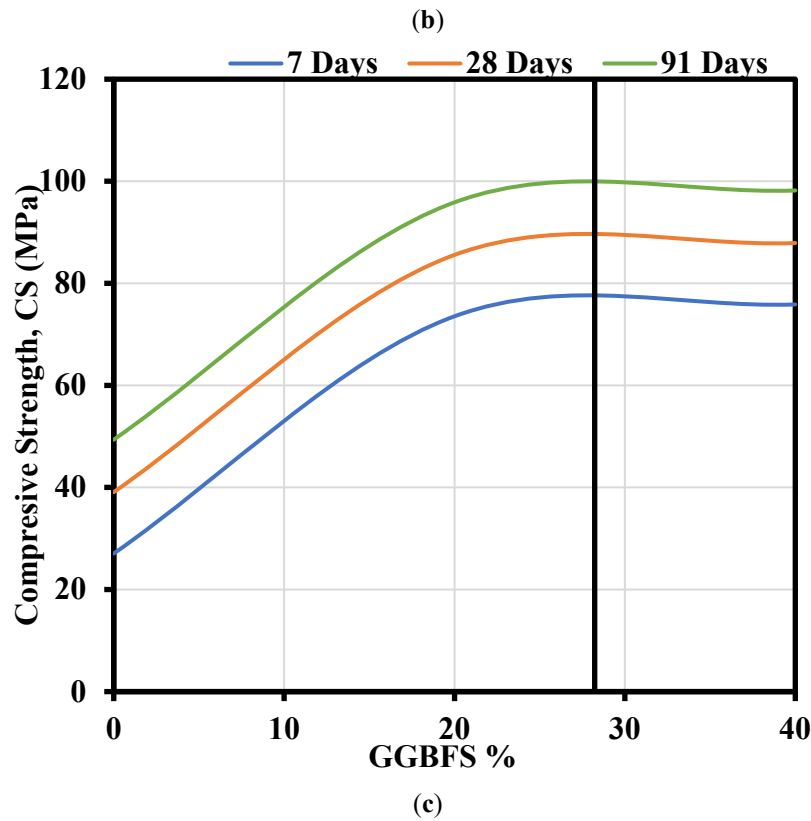


Figure 11. Comparison of compressive strength of concrete at 7, 28, and 91 days for different percentages of GGBFS using: (a) minimum content of cement, MRP, fine aggregate, and coarse aggregate; (b) average content of cement, fine aggregate, and coarse aggregate; (c) maximum content of cement, fine aggregate, and coarse aggregate.

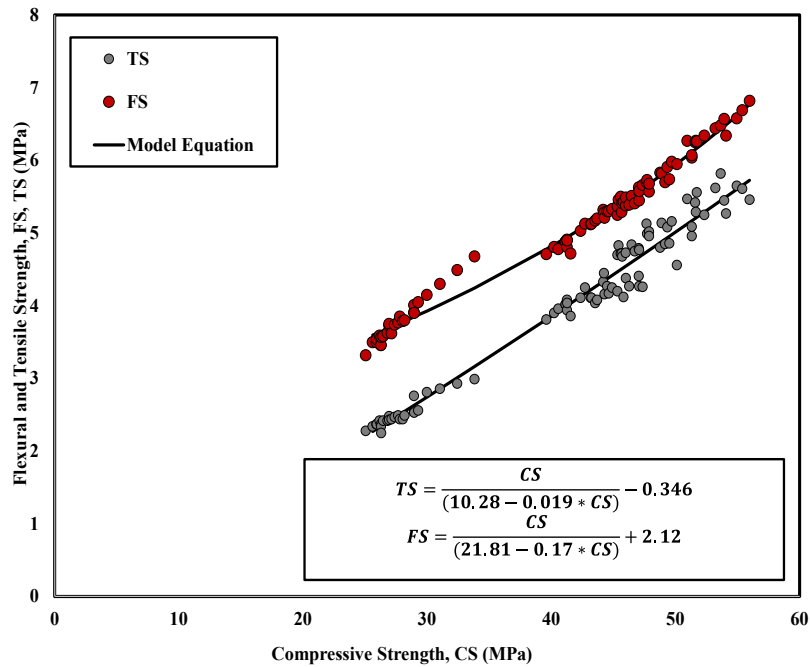


Figure 12. Correlation between compressive strength, CS (MPa) with each of tensile strength, TS (MPa) and flexural strength, FS (MPa).

In previous calculations, a pattern emerged: the optimum compressive strength of GGBFS-MRP-based concrete was achieved at extended curing periods and higher GGBFS replacement levels. Additionally, it was noted that lower water-to-binder (W/B) ratios result in higher compressive strength, consistent with a previous study that found a negative correlation between W/B and compressive strength in both ordinary concrete and high-volume slag concrete [34].

8. Limitations of the Study

- The dataset used was relatively small and specific, which limits the generalizability of the models to other concrete formulations.
- The validation process mainly relied on performance metrics without using advanced validation techniques like cross-validation, affecting the assessment of model robustness.
- Limited interpretability of feature effects was provided, mostly through sensitivity analysis, without employing more advanced interpretability tools such as SHAP or LIME.
- Potential overfitting issues in the ANN model were not thoroughly examined with validation plots or other methods.
- Future studies should expand the dataset to include a wider range of mix proportions and environmental conditions.
- The implementation of rigorous validation techniques, such as k-fold cross-validation, is recommended to ensure more reliable model assessment.
- Exploring advanced interpretability methods can yield better insights into feature importance.
- Applying these models to real-world concrete scenarios and predicting additional properties could improve practical applicability.

9. Conclusions

This study developed five statistical models to predict the compressive strength (CS) of concrete containing GGBFS and MRP. The sensitivity analysis indicated that curing time (18.33%), GGBFS content (2.36%), and MRP dosage (2.07%) were the most influential factors affecting CS. In contrast, the effects of cement, fine aggregate (FA), coarse aggregate (CA), and water-to-binder ratio (W/B) were negligible, with impact values of 0.66, 0.65, 0.60, and 0.32, respectively. Among the evaluated models, the Artificial Neural Network (ANN) demonstrated the highest predictive accuracy for CS of GGBFS-MRP concrete.

- (1) Based on the dataset and analysis results, the following conclusions were drawn:
- (2) The dataset included 0%, 20%, and 40% GGBFS replacement and 0%, 2.5%, and 5% MRP replacement. Increasing the GGBFS and MRP contents, along with an extended curing time, resulted in higher compressive strength.
- (3) Model performance was assessed using R^2 , RMSE, and MAE. The ANN model achieved optimal values with an R^2 of 0.999, an RMSE of 0.28 MPa, and an MAE of 0.23 MPa on the testing dataset.
- (4) The ANN model exhibited the lowest OBJ values (0.19 MPa for training, 0.08 MPa for testing) and lowest SI values (0.0078 for training, 0.0073 for testing), outperforming all other models.
- (5) Curing time, GGBFS content, and MRP dosage were identified as the most critical parameters influencing the prediction of compressive strength in GGBFS-MRP concrete.

Author Contributions

Z.R. and Z.M.: conceptualization, methodology, software; Z.B.: data curation, writing—original draft preparation; A.S.M.: visualization, investigation; A.S.M.: supervision; Z.B.: validation. All authors have read and agreed to the published version of the manuscript.

Funding

This research received no external funding.

Data Availability Statement

The data supporting the conclusions of this article are included with the article (<https://www.sciencedirect.com/org/science/article/pii/S2164632522002323> (accessed on 5 November 2025), https://docs.google.com/spreadsheets/d/1C_GoU6KQQxZQ8nNP86J3MyFp8-B7gxPg/edit?usp=sharing&oid=100315148316864473927&rtopf=true&sd=true (accessed on 5 November 2025)).

Conflicts of Interest

The authors declare no conflict of interest. Given the role as Editorial Board Members, Ahmed Salih Mohammed had no involvement in the peer review of this paper and had no access to information regarding its peer-review process. Full responsibility for the editorial process of this paper was delegated to another editor of the journal.

Use of AI and AI-Assisted Technologies

The authors utilized OpenAI ChatGPT-4o to enhance readability during the preparation of this work. They thoroughly reviewed and edited all content generated by these tools and take full responsibility for the final version of the published article.

References

1. Madloul, N.A.; Saidur, R.; Hossain, M.S.; et al. A Critical Review on Energy Use and Savings in the Cement Industries. *Renew. Sustain. Energy Rev.* **2011**, *15*, 2042–2060. <https://doi.org/10.1016/j.rser.2011.01.005>.
2. Soria, A.; Szabó, L.; Feroso, E.G.; et al. Energy Consumption and CO₂ Emissions from the World Cement Industry. In *JRC Science for Policy Report*; European Commission, Joint Research Centre: Luxembourg, 2016.
3. Penttala, V. Concrete and sustainable development. *ACI Mater. J.* **1997**, *94*, 409–416.
4. Mhaya, A.M.; Abidin AR, Z.; Sarbini, N.N.; et al. Role of Crumb Tyre Aggregates in Rubberised Concrete Contained Granulated Blast-Furnace Slag. *IOP Conf. Ser. Earth Environ. Sci.* **2019**, *220*, 012029. <https://doi.org/10.1088/1755-1315/220/1/012029>.
5. Thomas, B.S.; Gupta, R.C. A Comprehensive Review on the Applications of Waste Tire Rubber in Cement Concrete. *Renew. Sustain. Energy Rev.* **2016**, *54*, 1323–1333. <https://doi.org/10.1016/j.rser.2015.10.092>.
6. Amiri, M.; Hatami, F.; Mohammadi Golafshani, E. Evaluating Simultaneous Impact of Slag and Tire Rubber Powder on Mechanical Characteristics and Durability of Concrete. *J. Renew. Mater.* **2022**, *10*, 2155–2177. <https://doi.org/10.32604/jrm.2022.019726>.
7. Press, W.H.; Teukolsky, S.A.; Vetterling, W.T.; et al. Statistical Description of Data (Chap. 14, pp. 721–726). In *Numerical Recipes: The Art of Scientific Computing*, 3rd Ed.; Cambridge University Press: Cambridge, UK, 2007.
8. Khan, K.; Iqbal, M.; Jalal, F.E.; et al. Hybrid ANN models for durability of GFRP rebars in alkaline concrete environment using three swarm-based optimization algorithms. *Constr. Build. Mater.* **2022**, *352*, 128862.
9. Ahmed, H.U.; Mohammed, A.S.; Faraj, R.H.; et al. Compressive strength of geopolymer concrete modified with nano-silica: Experimental and modeling investigations. *Case Stud. Constr. Mater.* **2022**, *16*, e01036. <https://doi.org/10.1016/j.cscm.2022.e01036>.
10. Rahimzadeh, C.Y.; Salih, A.; Barzinjy, A.A. Systematic Multiscale Models to Predict the Compressive Strength of Cement Paste as a Function of Microsilica and Nanosilica Contents, Water/Cement Ratio, and Curing Ages. *Sustainability* **2022**, *14*, 1723. <https://doi.org/10.3390/su14031723>.
11. Qu, K. Research on linear regression algorithm. *MATEC Web Conf.* **2024**, *395*, 01046. <https://doi.org/10.1051/mateconf/202439501046>.
12. Khademi, F.; Jamal, S.M.; Deshpande, N.; et al. Predicting the compressive strength of ready mix concrete using a hybrid data-intelligence model. *Constr. Build. Mater.* **2017**, *138*, 805–815. <https://doi.org/10.1016/j.conbuildmat.2017.02.164>.
13. Hariaji, J. *Simple Linear Regression (SLR) Model and Multiple Linear Regression (MLR) Model*; Faculty of Mathematics and Natural Science State University of Medan: Medan, Indonesia, 2021.
14. Tranmer, M.; Murphy, J.; Elliot, M.; et al. *Multiple Linear Regression*, 2nd Ed.; Cathie Marsh Institute Working: Manchester, UK, 2020.
15. Qamar, R.; Zardari, B.A. Artificial neural networks: An overview. *Mesopotamian J. Comput. Sci.* **2023**, *2023*, 124–133. <https://doi.org/10.58496/MJCSC/2023/015>.
16. Mann, S.; Singh, G. Application of M5P Model Tree and Artificial Neural Networks for Traffic Noise Prediction on Highways of India. *Civ. Environ. Eng. Rep.* **2024**, *34*, 45–62. <https://doi.org/10.59440/ceer/188375>.
17. Ali, I.; Suthar, M. Comparison between Random forest and M5P to predict the compressive strength of concrete modified with solid wastes. *IOP Conf. Ser. Earth Environ. Sci.* **2023**, *1110*, 012085. <https://doi.org/10.1088/1755-1315/1110/1/012085>.
18. Chicco, D.; Warrens, M.J.; Jurman, G. The Coefficient of Determination R-squared Is More Informative than SMAPE, MAE, MAPE, MSE and RMSE in Regression Analysis Evaluation. *PeerJ Comput. Sci.* **2021**, *7*, e623. <https://doi.org/10.7717/peerj-cs.623>.
19. Jierula, A.; Wang, S.; Oh, T.M.; et al. Study on Accuracy Metrics for Evaluating the Predictions of Damage Locations in Deep Piles Using Artificial Neural Networks with Acoustic Emission Data. *Appl. Sci.* **2021**, *11*, 2314. <https://doi.org/10.3390/app11052314>.
20. Wang, W.; Lu, Y. Analysis of the Mean Absolute Error (MAE) and the Root Mean Square Error (RMSE) in Assessing Rounding Model. *IOP Conf. Ser. Mater. Sci. Eng.* **2018**, *324*. <https://doi.org/10.1088/1757-899x/324/1/012049>.
21. Bhattacharya, D.; Sinha, N. Scatter Index: An Alternative Measure of Dispersion Based on Relative Frequency of Occurrence of Observations. In *Lecture Notes in Networks and Systems, Proceedings of the 5th ICICC 2021, Bhubaneswar, India, 29–30 January 2022*; Springer: Singapore. https://doi.org/10.1007/978-981-19-1559-8_7.

22. Hasanah, U.; Putrawangsa, S.; Kumoro, D.T. Applying Linear Programming in Business Decision Making: A Case of Profit Maximization of a Commercial Housing Development. *Eur. J. Bus. Manag.* **2019**, *11*, 19. <https://doi.org/10.7176/ejbm/11-19-06>.
23. Emad, W.; Salih Mohammed, A.; Kurda, R.; et al. Prediction of concrete materials compressive strength using surrogate models. *Structures* **2022**, *46*, 1243–1267. <https://doi.org/10.1016/j.istruc.2022.11.002>.
24. Robeson, S.M.; Willmott, C.J. Decomposition of the mean absolute error (MAE) into systematic and unsystematic components. *PLoS ONE* **2023**, *18*, e0279774. <https://doi.org/10.1371/journal.pone.0279774>.
25. Jaf, I. Soft Computing and Machine Learning-Based Models to Predict the Slump and Compressive Strength of Self-Compacted Concrete Modified with Fly Ash. *Sustainability* **2023**, *15*, 11554. <https://doi.org/10.3390/su151511554>.
26. Asteris, P.G.; Apostolopoulou, M.; Armaghani, D.J.; et al. On the metaheuristic models for the prediction of cement-metakaolin mortars compressive strength. *Metaheuristic Comput. Appl.* **2020**, *1*, 63–99.
27. Pan, Y.; Wang, L.; Zhang, D. Effect of curing time on the mechanical properties of blended cementitious materials. *Constr. Build. Mater.* **2022**, *334*, 127445. <https://doi.org/10.1016/j.conbuildmat.2022.127445>.
28. Sadek, D.M. Influence of curing regimes on compressive strength development of eco-concrete. *J. Clean. Prod.* **2024**, *407*, 137228.
29. Rokhsana, S.; Uddin, M.; Ahmed, T. Utilization of GGBFS in concrete: A review on strength and durability. *Mater. Today Proc.* **2024**, *80*, 1480–1486.
30. Kumar, R.; Prasad, B.K. Performance evaluation of GGBFS-based concrete mixes under different curing regimes. *J. Sustain. Cem. Based Mater.* **2023**, *12*, 66–79.
31. Zhao, Y.; Huang, J.; Wu, B. Effect of recycled mineral powder on mechanical properties of blended cement mortar. *J. Mater. Civ. Eng.* **2021**, *33*, 04021088.
32. Ali, S.F.; Mahmood, T.; Khan, A. Utilization of mineral powders as cement replacement: Influence on strength and microstructure. *Case Stud. Constr. Mater.* **2022**, *16*, e00950.
33. Hatami, F.; Amiri, M. Experimental study of mechanical properties and durability of green concrete containing slag, waste rubber powder and recycled aggregate with artificial neural network. *Clean. Mater.* **2022**, *5*, 100112. <https://doi.org/10.1016/j.clema.2022.100112>.
34. Turumella, V.; Sravana, P.; Srinivasa, P. On the relationship between compressive strength and water binder ratio of high volumes of slag concrete. *Int. J. Appl. Eng. Res.* **2016**, *11*, 1436–1442.